

Bioinspired Mononuclear Mn Complexes for O₂ Activation and Biologically Relevant Reactions

Emma N. Cook and Charles W. Machan*

* - machan@virginia.edu; ORCID 0000-0002-5182-1138

E.N.C. ORCID 0000-0002-0568-3600

Department of Chemistry, University of Virginia, PO Box 400319, Charlottesville, VA 22904-4319

Abstract

A general interest in harnessing the oxidizing power of dioxygen (O₂) continues to motivate research efforts on bioinspired and biomimetic complexes to better understand how metalloenzymes mediate these reactions. The ubiquity of Fe- and Cu- based enzymes attracts significant attention and has resulted in many noteworthy developments for abiotic systems interested in direct O₂ reduction and small molecule activation. However, despite the existence of Mn-based metalloenzymes with important O₂-dependent activity, there has been comparatively less focus on the development of these analogues relative to Fe- and Cu- systems. In this *Perspective*, we summarize important contributions to the development of bioinspired mononuclear Mn complexes for dioxygen activation and studies on their reactivity, emphasizing important design parameters in the primary and secondary coordination spheres and outlining mechanistic trends.

Introduction

Dioxygen (O₂) is vital to aerobic life, playing critical roles in biological energy conversion and biomolecule synthesis and transformation.^{1–4} Harnessing the oxidative power of O₂ is also crucial for the development of alternative energy technologies and a ‘green’ alternative to the capital-intensive production of commodity chemicals and the selective activation of highly stable C–H and C–C bonds.^{5–12}

The triplet ground state of O₂ regulates its kinetic feasibility as an oxidant: while O₂ can easily accept electrons, direct reactivity with closed-shell organic substrates is a spin-forbidden process.^{1,2,7,13} Partial reduction of O₂ generates a reactive oxygen species (ROS); the one-electron reduction of O₂ forms superoxide, which can disproportionate into equal amounts of hydrogen peroxide and O₂ or be reduced further into hydrogen peroxide or water.^{1,2,7} The intrinsic instability of ROS intermediates can make it difficult to control reaction selectivity, once O₂ has been partially reduced.

However, transition metals are uniquely equipped to activate O_2 and are widely employed by nature to catalyze challenging oxidative reactions involving O_2 .^{1,7} Transition metals with open-shell ground states can react with triplet oxygen and facilitate its partial reduction. In order to selectively direct the oxidizing power of O_2 , these systems avoid the kinetic penalties associated with activating closed-shell substrates by generating peroxide species, complexing the substrate to intermediate metal superoxides, or facilitating O–O bond cleavage to produce high-valent metal oxo species.¹³ For concerted proton-coupled electron transfer reactions involving O_2 (or the products of partial O_2 reduction) and transition metal ions, the process is primarily controlled through reaction driving force, given that the protons and electrons involved in these reactions can be spatially separated.^{14,15}

There are numerous examples of enzymes containing mononuclear active sites that activate O_2 for its transport, reduction, and for the oxidation of organic substrates. Some examples include cytochrome *c* oxidase, cytochrome P450s, hemoglobin, dioxygenases, lipoxygenases, and superoxide dismutase, among others.^{2,9,16–22} The relative bioavailability of iron and its inherent redox flexibility have contributed to its ubiquity in O_2 -dependent cofactors.¹ Copper is also commonly employed by nature in O_2 -activating enzymes, such as hemocyanin, catechol oxidase, tyrosinase, and others.^{18,23–25} As a consequence of the prevalence of iron and copper in O_2 -activating enzymes, the field of O_2 activation has been dominated by synthetic models of Fe- and Cu-containing active sites.^{8,26,27}

Mn-based complexes have gained increased attention as analogues of Fe-based systems, owing to the fact that both Fe and Mn prefer similar coordination geometries and have analogous redox flexibility.¹ This is evident in biological systems as well: a number of Mn-dependent analogues of Fe-dependent enzymes exist, including lipoxygenases, dioxygenases, and superoxide dismutase.^{1,28–30} Additionally, Mn-dependent enzymes are important for the breakdown of ROSs in humans (Mn-dependent superoxide dismutase), seed germination and protecting plants from fungal infections (oxalate oxidase), wood-decaying fungi (oxalate decarboxylase), and the oxidation of polyunsaturated fatty acids into hydroperoxides (Mn-dependent lipoxygenases).^{28,31–34} Further, Mn plays a critical role in the active site of the O_2 -evolving complex in photosystem II, where H_2O is oxidized to O_2 during photosynthesis and represents the source of the vast majority of the world's O_2 .^{35,36}

Despite the importance and prevalence of Mn in the activation of O_2 in nature, there has historically been significantly less focus on Mn-based systems in comparison to that of Fe and Cu. However, in recent decades, there has been a significant increase in the number of studies

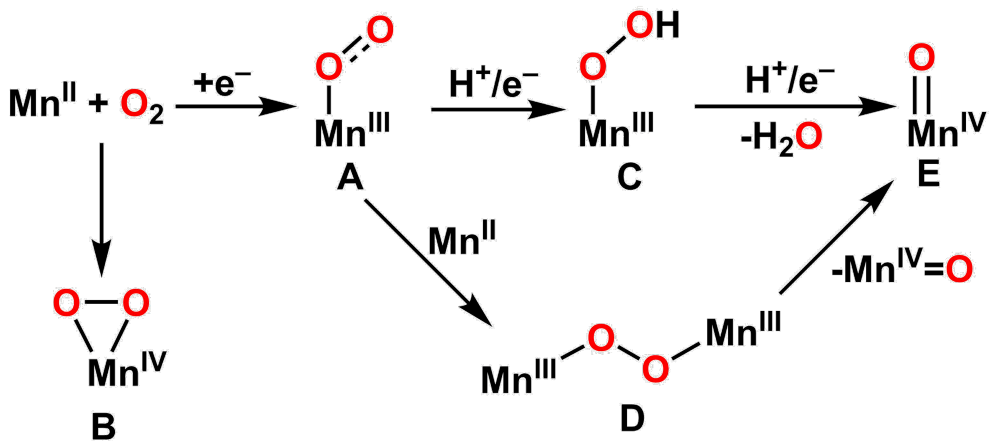
on Mn-based O_2 reactivity.^{37–44} Understanding the mechanisms in which O_2 is activated at discrete active sites is critical for the development of alternative energy technologies and catalysts for challenging C–H and C–C bond activation utilizing O_2 as an oxidant. In addition, biological models of these important enzymes will provide a foundation for the understanding of their structure and function in nature.

This *Perspective* will focus on recent advances in the development and study of bioinspired mononuclear non-heme Mn complexes that activate O_2 where the supporting ligand framework is not altered during activation, emphasizing the primary reactivity determinants of the active sites and describing the isolated high-valent oxygen-bound intermediates relevant to catalysis, as well as key challenges and opportunities for the area. Interested readers are directed to the following reviews and perspectives for discussion of O_2 activation by Mn porphyrin, corrole, and phthalocyanine complexes.^{1,4,11,45–49} The work of Duboc^{50–52} and Pecoraro^{34,53–56} focused on dinuclear manganese complexes for dioxygen activation should also be noted, as well as that of Anxolabéhère-Mallart on O_2 and H_2O activation at mononuclear non-porphyrinic Mn sites.^{57,58} Although beyond the intended scope, noteworthy related work by McKenzie and coworkers has described the activation of O_2 during oxygenation of the supporting ligand framework.⁵⁹ These examples and those detailed below have motivated our own work in the area of electrocatalytic reduction of O_2 with non-porphyrinic Mn complexes.^{60–62}

Reactivity of O_2 at Manganese

As introduced above, thermodynamically favorable oxidation reactions with O_2 can be made kinetically feasible through the use of transition metal centers.^{1,63} There are various possible pathways of O_2 activation at manganese, which are generalized in **Scheme 1**. O_2 can bind to the metal center (Mn^{II}) in an η^1 ‘end-on’ fashion, accompanied by formal electron transfer to generate a Mn–superoxide (O_2^{2-}) species (**A**) or in ‘side-on’ fashion to produce an η^2 -peroxy (O_2^{2-}) species (**B**).^{1,42,63,64} A transfer of one proton and one electron to **A** can lead to the formation of Mn–hydroperoxy ($-OOH$) species (**C**), which upon further protonation can lead to heterolytic or homolytic O–O bond cleavage and the formation of high valent Mn–oxo species (**E**).^{1,42,63} Alternatively, an additional equivalent of Mn^{II} can react with the Mn–superoxide species (**A**), forming a μ -peroxy dinuclear Mn species (**D**) that can undergo homolytic bond cleavage to form the high valent Mn–oxo species (**E**).^{1,42,63} These high-valent Mn–oxo species can be strong oxidants and, along with other the Mn-bound oxygen intermediate species, are important to the function of the aforementioned non-heme O_2 -activating Mn-dependent enzymes.^{65,66}

Scheme 1. Summary of Possible Reaction Pathways of O_2 at Mn



In weak-field ligand scaffolds, non-heme systems often lack the ligand σ -donating ability to stabilize the M–O₂ intermediates, making isolation and reactivity studies difficult.^{1,8,42} The mechanisms by which O₂ is activated at metalloproteins is controlled in part by the primary ligand coordination sphere, where the electronics of the metal center in the active site can be modulated,^{42,67–69} however, the secondary coordination sphere also plays an important role in the stabilization of reaction intermediates through hydrogen-bonding interactions.^{42,67–69}

Mononuclear Mn Complexes that Bind and Activate O₂

An important advancement in the study of O₂ binding at non-heme mononuclear Mn complexes was reported in 1997 by Borovik and coworkers, who showed that activation of O₂ at room temperature by a Mn^{II} complex resulted in the formation of an O₂-derived Mn^{III}–hydroxo species.³⁷ Borovik's group followed this initial study with additional reports on O₂ activation at Mn^{II} with urea-based tripodal ligand frameworks that can engage in hydrogen-bonding interactions with metal-bound O₂ and are poised for further reactivity (*vide infra*).^{38,39,68–71}

Inspired by the important role that Mn active sites play in photosynthesis and biological energy conversion, Kovacs and coworkers have made extensive progress in the understanding of O₂ activation at mononuclear nonheme Mn with their development of thiolate-ligated Mn^{II} complexes that bind O₂.^{40–42,72} Introduction of a thiolate into the inner coordination sphere provides a spectroscopic handle, attributed to the RS → M charge transfer (CT) band, that can be used to monitor the progress of the reaction. Indeed, the shifting of the RS → M CT band from the UV to visible region has been correlated to the formation of a lower energy metal-centered orbitals upon oxidation by O₂ binding, placing them closer in energy to the π -symmetric sulfur orbitals. This lowering in energy also provides electronic stabilization of Mn–O₂ species and decreases the activation barrier for O₂ binding.^{41–43} Kovacs' Group has also shown that modification of this initial

ligand design can have a profound influence on the reactivity of O_2 at Mn^{II} .⁴⁰⁻⁴³ In 2012, Kovacs and coworkers reported a series of thiolate-ligated Mn^{II} complexes (**Figure 1**, complexes **1-5**), where the ligand scaffold incorporated pendent pyridine moieties that can be synthetically modified in the 6-position to tune the electron-donating and steric profile of the ligand. These complexes were shown to react with O_2 , generating mono oxo-bridged Mn^{III} dimer species.⁴⁰ Follow-up studies were conducted to better understand the reactivity of O_2 at the methyl-substituted Mn^{II} complex (complex **1**), which resulted in the first structurally characterized μ -peroxo Mn^{III} dimer complex.⁴¹ Low-temperature kinetic studies revealed a mechanism of O_2 reactivity at **1**, where the mononuclear Mn^{III} - O_2 species that is formed upon exposure of **1** to O_2 reacts with an equivalent of **1** to yield the μ -peroxo Mn^{III} dimer species.⁴¹

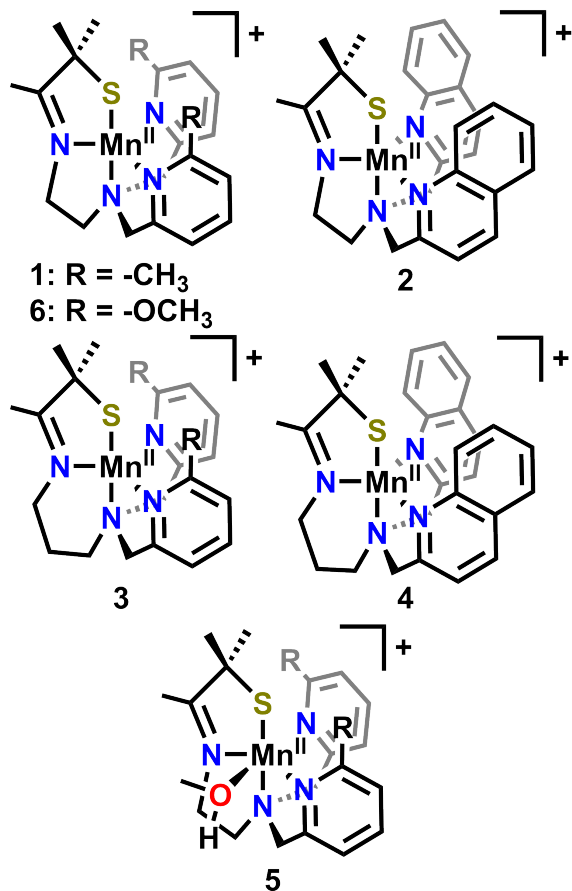


Figure 1. Structures of $[Mn^{II}(S^{Me2}N_4(6-R-DPEN))]^+$ $[Mn^{II}(L^{Rpy})]^+$ (top, left), $[Mn^{II}(S^{Me2}N_4(2\text{-QuinoEN}))]^+$ (top, right), $[Mn^{II}(S^{Me2}N_4(6\text{-Me-DPPN}))]^+$ (middle, left), $[Mn^{II}(S^{Me2}N_4(2\text{-QuinoPN}))]^+$ (middle, right) and $[Mn^{II}(S^{Me2}N_4(6\text{-H-DPEN})(MeOH))]^+$ (bottom) reported by Kovacs and coworkers.

By modifying the steric profile at the 6-position, Kovacs and coworkers have correlated the mean Mn–N distance of the pendent pyridine fragments in these Mn complexes (**Figure 1, 1–4**) with the kinetic barrier for alkylperoxy O–O bond cleavage, finding that sterically hindered ligands prevented optimal Mn–N bond distance and result in a more Lewis acidic metal ion.⁷² More Lewis acidic metal ions lead to a stronger π -interaction with O_2 , by shifting electron density out of the peroxy $\pi^*(O-O)$ manifold into the Mn–O π -bonding interaction, strengthening the O–O bond. Alternatively, less Lewis acidic metal centers (more electron-rich Mn center) have a weaker π -interaction with O_2 , as a result of donating electron density from their π -symmetric metal orbitals into the peroxy π^* manifold, weakening the O–O bond and making cleavage kinetically feasible.⁷² In a 2019 report on O_2 activation at analogous Mn complexes, they undertook a comprehensive study focused on metal ion Lewis acidity and ligand sterics, elucidating a mechanism for O_2 binding and O–O bond cleavage at a series of Mn^{II} complexes ($[Mn^{II}(S^{Me_2}N_4(6-Me-DPEN))]^+$ (**1**), $[Mn^{II}(S^{Me_2}N_4(2-QuinoEN))]^+$ (**2**), $[Mn^{II}(S^{Me_2}N_4(6-OMe-DPEN))]^+$ (**6**)).⁴³ They found that O_2 binding to Mn^{II} is less favored for the less Lewis acidic complexes (**6, 2**) in comparison to complex **1**, with O_2 release from the superoxo species derived from these complexes being more favorable than the generation of the mono oxo bridged dimanganese complex.⁴³ Additionally, they found a strong correlation between the Mn^{III/II} redox potential and the ligand-dependent activation barrier to O_2 binding and conversion of Mn superoxo species to peroxy states.⁴³ Finally, dinuclear Mn bridging peroxy and oxo intermediates of the more electron donating, less sterically encumbered derivative (**6**), were observed where the bridging oxo species were shown to cleave strong X–H bonds.⁴³

In an independent effort to mimic the reactivity at Mn-dependent enzymes, Jackson and coworkers have synthesized Mn^{II} complexes supported by pentadentate amide-containing ligands that react with O_2 to yield Mn^{III}–hydroxo adducts.⁴⁴ Their 2019 report described the divergent reaction pathways of O_2 at $[Mn^{II}(dpaq)]^+$ (**7**) and a sterically modified derivative, $[Mn^{II}(dpaq^{2Me})]^+$ (**8**) (**Figure 2**).⁴⁴ O_2 titration experiments revealed a difference in reaction stoichiometries where **7** reacts with a Mn: O_2 ratio of 4:1 and **8** reacts in a 2:1 ratio, suggesting differing reaction pathways, which are summarized in **Scheme 2**.⁴⁴ Both **7** and **8** react with O_2 to produce a peroxydimanganese(III,III) species that undergoes homolytic O–O bond cleavage to form high-valent mononuclear Mn^{IV}–oxo or a bis(μ -oxo)dimanganese(IV) dimer. The high-valent Mn^{IV}–oxo species of complex **7** can undergo comproportionation with **7** in solution to form a (μ -oxo)dimanganese(III,III) species that is hydrolyzed to Mn^{III}–OH in the presence of water. However, due to the steric bulk of the modified ligand in complex **8**, comproportionation of Mn^{IV}–oxo and formation of a bridging oxo dimanganese species is disfavored. This leads to the Mn^{IV}–

oxo complex abstracting a hydrogen atom from MeCN, forming $\text{Mn}^{\text{III}}\text{--OH}$. This was further confirmed through the incorporation of deuterium in $d_3\text{-MeCN}$, forming $\text{Mn}^{\text{III}}\text{--OD}$ as the product. These results suggest that the introduction of a methyl group in the 2-position of the quinoline moiety of the ligand disfavors the formation of the bridged-oxo dimer, allowing access to a divergent reaction pathway for complex **8**.⁴⁴

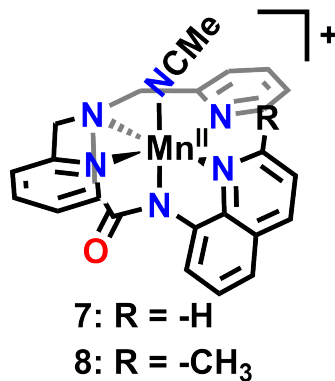
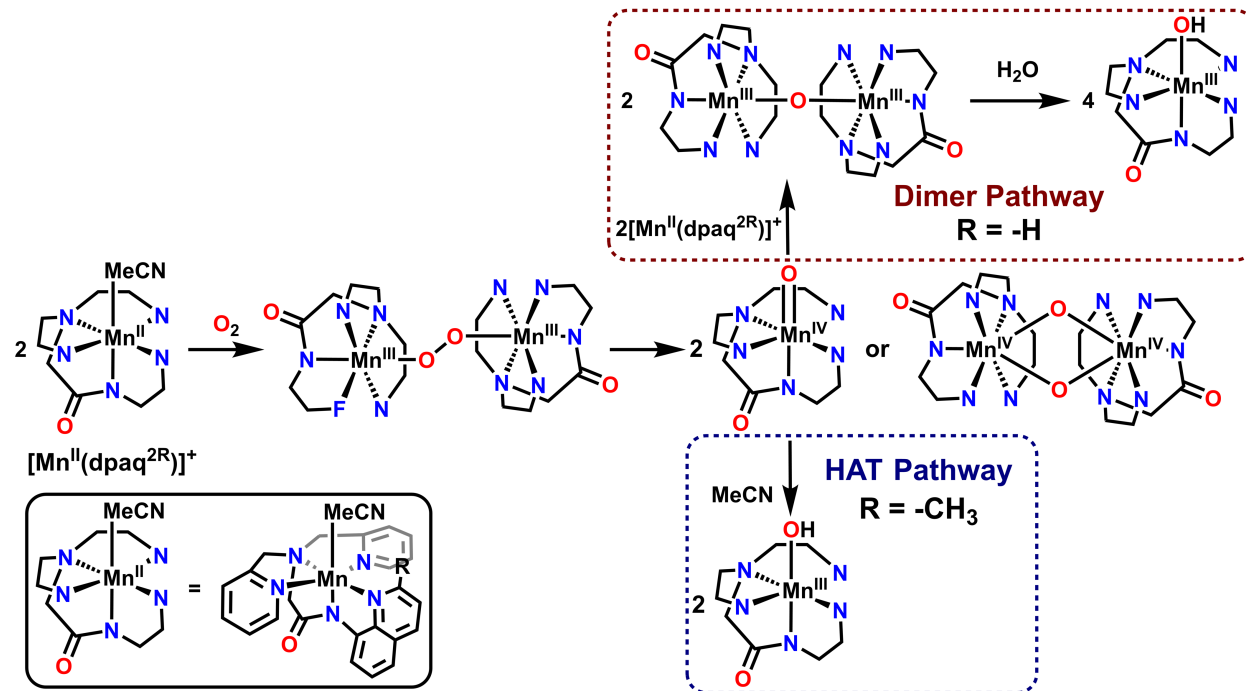


Figure 2. Structure of $[\text{Mn}^{\text{II}}(\text{dpaq}^{\text{R}})]^+$ reported by Jackson and coworkers.⁴⁴

Scheme 2. Summary of reaction pathways by complexes **7** and **8** from ref. 44.



High-Valent Mn–O Intermediates Critical to O₂ Activation – Advances in Characterization and Reactivity

Manganese-oxygen (Mn–O[H] or Mn–O₂[H]) species have been proposed as key intermediates for many biological processes involving the activation of O₂. For example, Mn-lipoxygenase

invokes a Mn^{III}–OH intermediate to abstract a hydrogen atom from a polyunsaturated fatty acid substrate.⁷³ Mn–oxo species are suggested to be important intermediates during photosynthetic water splitting mediated by the oxygen evolving complex in photosystem II.^{17,73,74} A Mn–peroxo intermediate is important to the function of manganese superoxide dismutase, which converts superoxide into a half equivalent each of hydrogen peroxide and O₂.^{32,73} Understanding these key intermediates and their reactivity is important for the development of biomimetic systems and harnessing them for direct reduction or the activation of C–H and C–C bonds.

The Borovik group has made extensive progress in the development of Mn complexes with ligand-stabilized hydroxo and oxo ligands in order to better understand reactivity of biologically relevant intermediates.^{39,68,70,71,74–82} Motivated by efforts to understand biological hydrogen atom transfer (HAT) processes, Borovik and coworkers developed monomeric manganese complexes with terminal hydroxo ligands. The urea-based ligand framework used in these studies inhibits bridging coordination modes for the hydroxide ions and provides control over secondary coordination sphere interactions through the creation of a well-defined intramolecular hydrogen-bonding pocket around the Mn–O(H) core (**Figure 3**).^{68,71,78} Using this structural paradigm, Borovik and coworkers have elucidated the bond dissociation energies of Mn^{III}–OH complexes and corroborated these findings with HAT reactivity across a variety of substrates.⁷⁹ In subsequent studies, the Borovik group established the preparation and structural and spectroscopic properties of a new class of stabilized Mn^{III}, Mn^{IV}, and Mn^V–O and –OH complexes.^{37,74–76,79,80} The use of this tripodal ligand framework has been important to the development of biomimetic Mn–hydroxo/oxo complexes and for establishing an understanding of the reactivity of these complexes and the secondary coordination sphere in the context of biological processes.^{39,68,70,71}

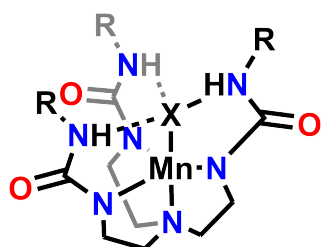


Figure 3. Generalized structure of urea-based [H₃buea]³⁻ ligand framework developed by Borovik and coworkers, X = O, OH and R = ^tBu.

Recently, Borovik and coworkers have studied the effects of the basicity of Mn–oxo complexes on C–H bond cleavage reactions. Their previously reported urea-based ligand scaffold was modified to replace a ^tBu group with a para-substituted phenyl group on one HN_{urea} unit (**Figure**

4).⁷⁷ This design was employed to control hydrogen-bonding strength with the HN_{urea} groups and $\text{Mn}^{\text{III}}\text{-oxo}$ to tune the oxo ligand basicity.⁷⁷ As the substituent electron-withdrawing ability is increased, adjacent HN_{urea} groups form stronger H-bonds with the $\text{Mn}^{\text{III}}\text{-oxo}$, leading to a decrease in oxo ligand basicity. To understand C–H bond activation dependence on $\text{Mn}^{\text{III}}\text{-oxo}$ basicity (its Mn-OH analogue), six complexes (**Figure 4**, $[\text{Mn}^{\text{III}}\text{H}_3\text{bpuea-R(O)}]^{2-}$, **9-13** and $[\text{Mn}^{\text{III}}\text{H}_2\text{bpuea-5F(OH)}]^{2-}$, **14**) were synthesized and their reactivity with 9,10-dihydroanthracene (DHA), xanthene, and fluorene was analyzed.⁷⁷ They found that under anaerobic conditions complexes **9-13** activated dihydroanthracene (DHA), resulting in the formation of anthracene (**Eq. 1**).⁷⁷ A correlation between $\text{Mn}^{\text{III}}\text{-oxo}$ basicity and second-order rate constants for the activation of DHA was observed, where the most basic $\text{Mn}^{\text{III}}\text{-oxo}$ complex (**9**) had the largest rate constant.⁷⁷ Further, the reaction rates did not trend with $\text{BDFE}_{\text{O-H}}$ of the product $\text{Mn}^{\text{II}}\text{-OH}$, which was constant across the series of complexes.⁷⁷ Reactivity studies with fluorene and xanthene were also completed to examine a substrate series with varied $\text{p}K_{\text{a}}$ and $\text{BDFE}_{\text{C-H}}$ values. Complexes **9**, **10**, and **12** were only able to deprotonate fluorene. Additionally, complexes **9**, **10**, and **12** were able to cleave C–H bonds in xanthene, but significantly faster than DHA.⁷⁷ These data suggest that $\text{p}K_{\text{a}}$ rather than $\text{BDFE}_{\text{O-H}}$ of $\text{Mn}^{\text{II}}\text{(O-H)}$ is an important determinant in their reactivity toward C–H bonds. However, due to the increase in reaction rate with xanthene and large ΔS^{\ddagger} values obtained from Eyring analysis, the mechanism of C–H bond cleavage by these $\text{Mn}^{\text{III}}\text{-oxo}$ complexes is more convoluted than a simple proton transfer/electron transfer.⁷⁷ Formation of the $\text{Mn}^{\text{II}}\text{-OH}$ species upon C–H bond cleavage can occur by a proton-coupled electron transfer (PCET, **Figure 5**), where formal proton transfer (PT, dependent on $\text{p}K_{\text{a}}$ of the protonated product) is followed by an electron transfer (ET, dependent on reduction potential $E_{1/2}$), or vice versa, or in a concerted fashion (concerted proton-electron transfer, CPET), where PT and ET happen synchronously to form the product. Based on these data, the authors proposed an asynchronous mechanism for concerted proton and electron transfer to the $\text{Mn}^{\text{III}}\text{-oxo}$ unit at the transition state.^{77,83}

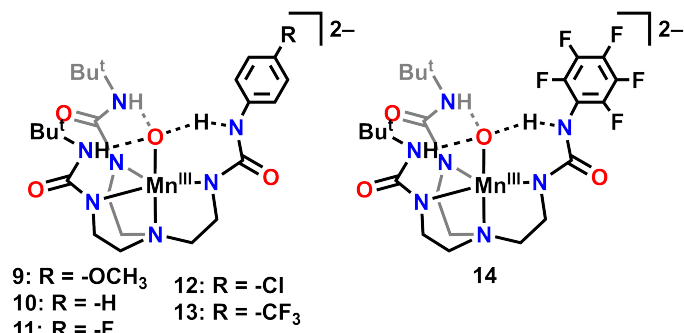


Figure 4. Structures of $[\text{Mn}^{\text{III}}\text{H}_3\text{bpuea}-\text{R}(\text{O})]^{2-}$ (left) and $[\text{Mn}^{\text{III}}\text{H}_2\text{bpuea}-5\text{F}(\text{OH})]^{2-}$ reported by Borovik and coworkers.⁷⁷

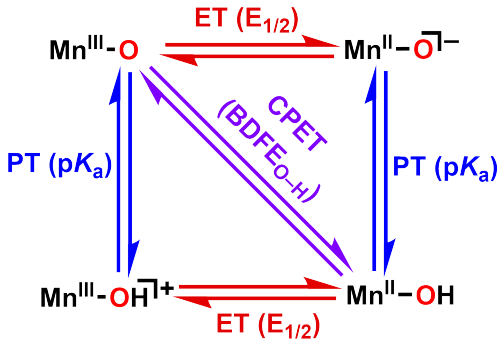
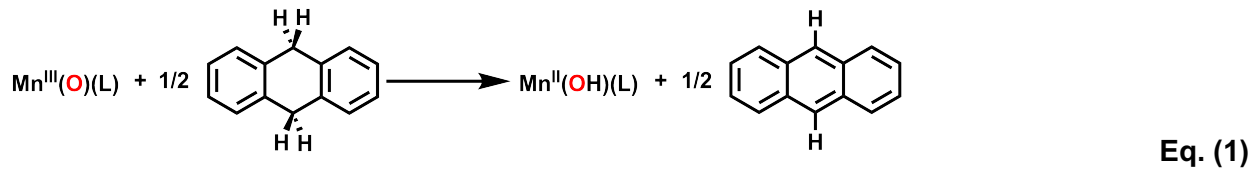


Figure 5. Square scheme summarizing PCET reactivity of complexes **9-13** during HAT with DHA.

The Jackson group has also made significant contributions to the understanding of Mn–O₂ reactivity.^{84–96} In 2016, Jackson and coworkers elucidated the electronic structure a Mn^{IV}–oxo complex supported by a pentadentate N₅ ligand scaffold, [Mn^{IV}(O)(N4py)]²⁺ (**Figure 6**, complex **15**). Using electronic absorption and magnetic circular dichroism (MCD) experiments, supplemented with density functional theory (DFT) and CASSCF computations, they were able to spectroscopically identify the low-lying quartet excited state previously proposed by Nam and Shaik as central to the HAT and OAT reactivity of **15**.^{93,97} In follow-up work, Jackson and coworkers sought to further understand the influence of the excited state energy of Mn^{IV}–oxo complexes on the rate of HAT and OAT by altering equatorial ligand field strength.⁹⁴ Mn^{IV}–oxo complexes **16** and **17** include incorporation of sterically bulky quinolinyl (2pyN2Q) and electron-rich 3,4-dimethyl-5-methoxypyridyl (^{DMM}N4py)) groups onto the N4py ligand scaffold, where the equatorial field is strengthened and weakened relative to N4py, respectively (**Figure 6**).⁹⁴ Kinetic analysis of HAT reactivity with DHA, diphenylmethane, and ethylbenzene revealed a trend in second-order rate constants where the rate decreased as equatorial ligand field strength increased: **16** > **15** > **17**. OAT reactivity was analyzed through reaction of each Mn^{IV}–oxo complex with thioanisole, revealing a similar trend in rate constants with a 153- and 4000-fold increase in rate by **16** relative to **15** and **17**, respectively. Density functional theory (DFT) methods were used to corroborate structural and electronic information. These trends experimentally supported the dependence of HAT and OAT reactivity on the quartet excited state energy level, where its lowering as a result of weakening the ligand field strength increases the electrophilicity of the Mn^{IV}–oxo unit and causes faster rates of reactivity.⁹⁴

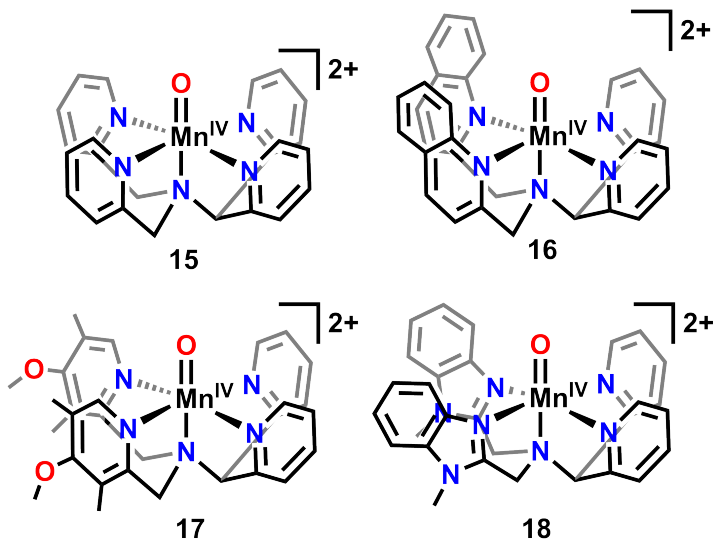


Figure 6. Structures of $[\text{Mn}^{\text{IV}}(\text{O})(\text{N}4\text{py})]^{2+}$ (top, left), $[\text{Mn}^{\text{IV}}(\text{O})(2\text{pyN}2\text{Q})]^{2+}$ (top, right), $[\text{Mn}^{\text{IV}}(\text{O})(^{\text{DMM}}\text{N}4\text{py})]^{2+}$ (bottom, right), $[\text{Mn}^{\text{IV}}(\text{O})(\text{N}2\text{py}2\text{B})]^{2+}$ (bottom, right) reported by Jackson and coworkers.^{93–95}

In subsequent studies, the Jackson group conducted additional studies to understand the underlying causes of OAT rate enhancement and mechanism for these Mn^{IV} -oxo complexes, including isolation of a new analogue (complex **18**, **Figure 6**) that further modified effective equatorial ligand field strength through the incorporation of benzimidazolyl groups (N2py2B) instead of pyridine derivatives.⁹⁵ The reaction rate of OAT was shown to increase as equatorial ligand field strength decreased, following a trend of **16** > **15** > **18** > **17**. Variable-temperature Eyring analysis of thioanisole sulfoxidation revealed large enthalpic barriers, which increased with increasing equatorial ligand field strength, indicating that reaction barriers are controlled by enthalpy of activation.⁹⁵ Although the observed small entropic contributions could be suggestive of a rate-limiting ET step, this possibility was excluded through a combination of Hammett Marcus analyses, which ruled out a two-step OAT mechanism with rate-limiting ET.⁹⁵ These data further support the proposal that OAT mediated by these Mn^{IV} -oxo complexes proceeds via a concerted ET/OAT step for all complexes and that rate enhancement is dependent on equatorial ligand field strength controlling the enthalpy of activation of thioanisole oxidation.

In addition, the Jackson group has also studied $\text{Mn}^{\text{III}}\text{–OH}$ complexes, derived from O_2 , that perform C–H bond activation.^{86,96} In 2014, they found that a $\text{Mn}^{\text{III}}\text{–OH}$ with a monoanionic N_5dpaq ligand (**Figure 7**, complex **19**), was able to oxidize xanthene and phenol derivatives, as well as catalytically oxidize TEMPOH by $[\text{Mn}^{\text{II}}(\text{dpaq})](\text{OTf})$ with O_2 in MeCN (**Eq. 2**).⁹⁶

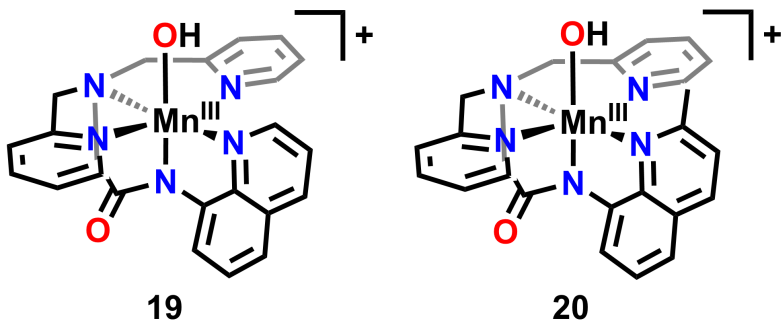
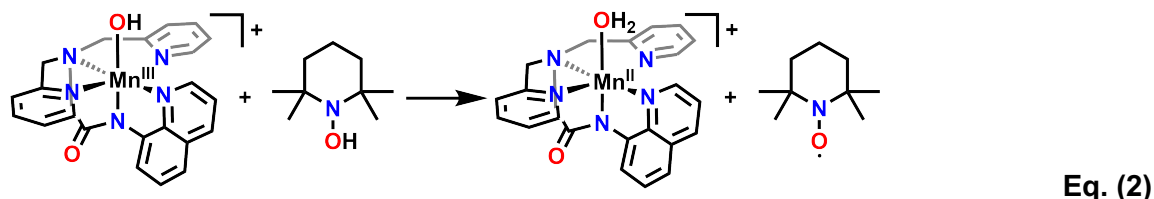


Figure 7. Structures of $[\text{Mn}^{\text{III}}(\text{OH})(\text{dpaq})]^+$ (left) and $[\text{Mn}^{\text{III}}(\text{OH})(\text{dpaq}^{2-\text{Me}})]^+$ (right) reported by Jackson and coworkers.^{86,96}



Kinetic analysis revealed a relatively low KIE with TEMPO–H/D of 1.8 suggests that O–H bond cleavage is rate limiting. These data, in combination with the low reduction potential of the active catalyst, $[\text{Mn}^{\text{III}}(\text{OH})(\text{dpaq})]^+$, suggest a CPET mechanism of TEMPOH oxidation.⁹⁶ Interestingly, saturation kinetics of oxidation of phenols by Mn^{III}–OH indicated an equilibrium step involving the formation of a hydrogen-bonded complex is followed by rate-limiting CPET to form Mn^{II}–OH₂ and phenol radical.⁹⁶

A follow-up study modified the dpaq ligand to incorporate a 2-methylquinoline moiety ($[\text{Mn}^{\text{III}}(\text{OH})(\text{dpaq}^{2-\text{Me}})]^+$, complex **20**), in order to introduce steric bulk at the equatorial position and perturb the metal electronic structure by weakening metal-ligand coordination (Figure 7).⁸⁶ The substituted complex **20** showed more rapid reactivity with TEMPOH in comparison to the non-substituted, but little to no rate enhancement was observed with bulkier substrates. Eyring analysis of TEMPOH oxidation by **20** revealed that activation energy decreased significantly with **20** in comparison to **19**.⁸⁶ The combination of kinetic and computation studies indicated that the introduction of the methyl group into the ligand framework modulated electronics of the Mn^{III}–OH unit and increased the thermodynamic driving force of TEMPOH oxidation. This was reflected by the $\text{BDFE}_{\text{O}-\text{H}}$ of the $[\text{Mn}^{\text{II}}(\text{OH}_2)(\text{dpaq}^{\text{R}})]^+$ product for R = 2Me being larger than R = H and more favorable reduction of $[\text{Mn}^{\text{III}}(\text{OH})(\text{dpaq}^{2\text{-Me}})]$ in comparison to $[\text{Mn}^{\text{III}}(\text{OH})(\text{dpaq})]$.⁸⁶

In subsequent studies, the dpaq ligand was modified in the 5-position on the quinolinyl unit with electron-donating and -withdrawing groups to establish structure-activity relationships for HAT reactivity in a series of $\text{Mn}^{\text{III}}\text{--OH}$ complexes (complexes **21**–**24**, **Figure 8**).⁸⁷ They found that although increasing the electron-withdrawing character of the quinolinyl substituent caused a corresponding increase in the rate of TEMPOH oxidation, the effect was relatively minor.⁸⁷ These results were attributed to the change of $\text{Mn}^{\text{III}/\text{II}}\text{--OH}$ redox potential induced by the change in ligand substituent, where the rate of PCET reactivity is dependent on the one-electron reduction potential and pK_a (**Figure 8**, bottom). The shallow dependence on electron-withdrawing ability of the ligand and rate of PCET was corroborated by computed pK_a values of $\text{Mn}^{\text{III}}\text{--OH}$ species, which suggested that $E_{1/2}$ values are compensated by changes in pK_a .⁸⁷

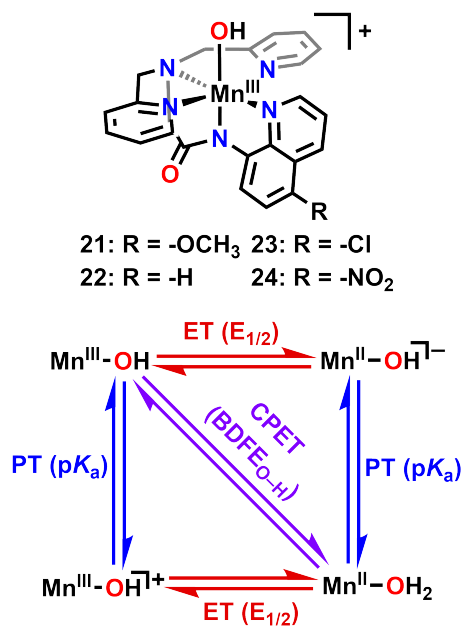


Figure 8. (top) Structure of $[\text{Mn}^{\text{II}}(\text{OH}_2)(\text{dpaq}^{\text{5R}})]^+$ reported by Rice et al. (bottom) square scheme depicting the PCET reactivity of $\text{Mn}^{\text{III}}\text{--OH}$ species during HAT.⁸⁷

Most recently, Jackson and coworkers employed a previously reported ligand framework ($[\text{Mn}^{\text{III}}(\text{OH})(\text{PaPy}_2\text{Q})]^+$, **25** **Figure 9**) and a synthetically modified derivative that provides a hydrogen-bonding interaction ($[\text{Mn}^{\text{III}}(\text{OH})(\text{PaPy}_2\text{N})]^+$, **26** **Figure 9**) and studied the dependence of oxidation reactions of TEMPOH and a variety of phenol derivatives.⁸⁸ They found that the rate of TEMPOH oxidation by complex **26** was 15-fold higher than for complex **25**. Thermodynamic and computational analyses were used to further understand the basis for this rate enhancement. The driving force for the CPET reaction between $\text{Mn}^{\text{III}}\text{--OH}$ and TEMPOH is dependent on the BDFE of the $\text{Mn}^{\text{II}}\text{--aqua}$ product and is reflected in a faster observed reaction rate for the complex whose $\text{Mn}^{\text{II}}\text{--aqua}$ product has a stronger O–H bond.⁸⁸ They attributed the difference in reaction rates by

25 and **26** to the difference in Mn^{II}–aqua BDFEs where **26** stabilizes the Mn^{II}–aqua complex through hydrogen bonding interactions that aren't available in **25**.⁸⁸ Jackson and coworkers also observed rate enhancements of phenol oxidation by **26** relative to **25**. This was also attributed to larger driving force due to stronger Mn^{II}–aqua O–H bonds that are stabilized in **26**.⁸⁸

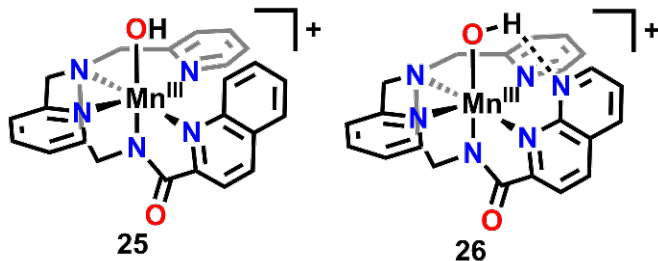


Figure 9. Structures of $[\text{Mn}^{\text{III}}(\text{OH})(\text{PaPy}_2\text{Q})]^+$ (left) and $[\text{Mn}^{\text{III}}(\text{OH})(\text{PaPy}_2\text{N})]^+$ reported by Jackson and coworkers.⁸⁸

Fukuzumi, Nam, and coworkers have also made important contributions to the study of high-valent Mn–O species and their reactivity in oxidation reactions.^{98–100} In 2018, they reported the first Mn^{III}–aqua complex $[\text{Mn}^{\text{III}}(\text{OH}_2)(\text{dpaq})]^{2+}$ (complex **27**) with high reactivity toward HAT involving substrate O–H and C–H bonds (Figure 10).⁹⁹ A subsequent 2021 report re-examined this Mn^{III}–aqua complex and its reactivity toward OAT with methoxy-substituted thioanisoles and triphenylphosphine derivatives in MeCN solution.¹⁰⁰ Mechanistic analysis showed that OAT from $[\text{Mn}^{\text{III}}(\text{OH}_2)(\text{dpaq})]^{2+}$ to thioanisoles and triphenylphosphine derivatives proceed via an outer-sphere electron transfer, supported by the observation that the second-order reaction rate constants of OAT were dependent on the oxidation potential of the substrate.¹⁰⁰

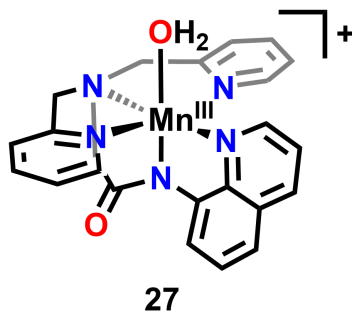
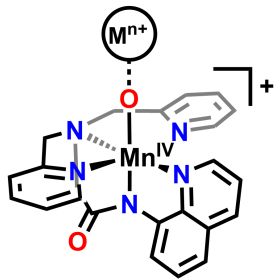


Figure 10. Structure of $[\text{Mn}^{\text{III}}(\text{OH}_2)(\text{dpaq})]^{2+}$ reported by Fukuzumi, Nam, and coworkers.^{99,100}

In addition, Fukuzumi, Nam, and coworkers have also studied the effects of redox-inactive metal ions binding at Mn(IV)–oxo complexes on the observed electron transfer, OAT reactivity with thioanisole, and HAT reactivity with 1,4-cyclohexadiene (Figure 11).¹⁰¹ Mn^{IV}–oxo complexes with

a series of redox-inactive metals bound ($[\text{Mn}^{\text{IV}}(\text{O})(\text{dpaq})]^+ - \text{M}^{\text{n}+}$, where $\text{M}^{\text{n}+} = \text{Ca}^{2+}$, Mg^{2+} , Zn^{2+} , Lu^{3+} , Y^{3+} , Al^{3+} , and Sc^{3+}) were synthesized using an oxygen atom donor and redox-inactive metal ion triflates. Without the addition of the redox-inactive $\text{M}^{\text{n}+}$ ions, the formation of a mixed-valent bis(μ -oxo)dimanganese(III,IV) complex was instead observed. It was found that electron transfer (ET), OAT, and HAT were dependent on $\text{M}^{\text{n}+}$ Lewis acidity: increasing the Lewis acidity of the redox-inactive ion $\text{M}^{\text{n}+}$ increases reactivity of the oxo unit $[(\text{dpaq})\text{Mn}^{\text{IV}}(\text{O})]^+ - \text{M}^{\text{n}+}$ toward OAT and ET but decreases reactivity toward HAT. These observations imply that the Lewis acidity of $\text{M}^{\text{n}+}$ controls the reduction potential and basicity of the $\text{Mn}^{\text{IV}}\text{-oxo}$ unit.¹⁰¹ The mechanism of OAT was found to be dependent on the rate of ET, followed by fast OAT, and can be controlled by modulating the reduction potential of the $[\text{Mn}^{\text{IV}}(\text{O})(\text{dpaq})]^+ - \text{M}^{\text{n}+}$. This is supported by the dependence of ET rate on $\text{M}^{\text{n}+}$ Lewis acidity, where stronger Lewis acids cause a more positive shift in the one-electron reduction potential and demonstrate faster ET. Using OAT sulfoxidation reactivity with thioanisole as a model reaction, a dependence on $\text{M}^{\text{n}+}$ Lewis acidity was observed where, as Lewis acidity increases, OAT reactivity increases due to its rate-limiting ET. The proposed mechanism of OAT was further corroborated by kinetic analysis of $[\text{Mn}^{\text{IV}}(\text{O})(\text{dpaq})]^+ - \text{Sc}^{3+}$ with *para*-substituted thioanisoles of varying electron-donating ability, which showed that as the electron-donating ability of the substrate increases, the rate of sulfoxidation increases and is indicative of ET being involved in the rate-limiting step.

However, HAT reactivity showed an opposite trend, where increasing the Lewis acidity of $\text{M}^{\text{n}+}$ resulted in a decrease in the rate of HAT. This was attributed to the change in basicity of the $\text{Mn}^{\text{IV}}\text{-oxo}$ unit where, as axial ligand ($\text{M}^{\text{n}+}$) electron-donating ability increases (Lewis acidity decreases), $\text{Mn}^{\text{IV}}\text{-oxo}$ basicity increases. This supports the trend that HAT reactivity by $[\text{Mn}^{\text{IV}}(\text{O})(\text{dpaq})]^+ - \text{M}^{\text{n}+}$ is limited by the rate of PT, followed by rapid ET. In a follow-up study, Karmalkar *et. al* examined $[\text{Mn}^{\text{IV}}(\text{O})(\text{dpaq})]^+ - \text{M}^{\text{n}+}$ adducts, where $\text{M}^{\text{n}+} = \text{Ce}^{4+}$, and the corresponding ET and OAT reactivity for comparison using cerium as a bound redox-active metal center.¹⁰² Kinetic analyses to observe the rate of ET from $[\text{Fe}^{\text{II}}(\text{Me}_2\text{bpy})_3]^{2+}$ and OAT with thioanisole derivatives (where the mechanism proceeds via rate-limiting ET) revealed that $[\text{Mn}^{\text{IV}}(\text{O})(\text{dpaq})]^+ - \text{Ce}^{4+}$ is a stronger oxidant in comparison to $[\text{Mn}^{\text{IV}}(\text{O})(\text{dpaq})]^+ - \text{M}^{\text{n}+}$, where $\text{M}^{\text{n}+} = \text{Ca}^{2+}$, Mg^{2+} , Zn^{2+} , Lu^{3+} , Y^{3+} , Al^{3+} , and Sc^{3+} .¹⁰²



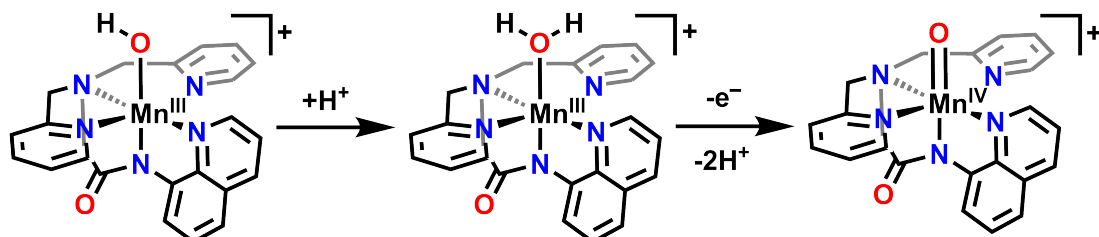
$M^{n+} = Ca^{2+}, Mg^{2+}, Zn^{2+},$
 $Lu^{3+}, Y^{3+}, Al^{3+}, Sc^{3+}, Ce^{4+}$

28

Figure 11. Structure of $Mn^{IV}(O)(dpaq)]^+-M^{n+}$ reported by Fukuzumi, Nam, and coworkers.^{101,102}

Soon after, Paul, Biswas and coworkers showed that an analogous high-spin Mn(IV)-oxo complex with a dpaq ligand framework was formed via a stepwise PCET reaction, without the addition of redox-inactive metals or an OAT agent (Scheme 3).¹⁰³ Using both $[Ru(bpy)_3]^{3+}$ and ceric ammonium nitrate (CAN) as one-electron oxidants and triflic acid (HOTf) as the proton donor, they formed transient $[Mn^{IV}(O)(dpaq)]^+$, confirming its formation through EPR, Raman, and UV-vis spectroscopic analyses and showed that protonation of the hydroxide species is crucial prior to further oxidation and rapid deprotonation of the resulting Mn^{III} -aqua species. HAT reactivity of $[Mn^{IV}(O)(dpaq)]^+$ with xanthene, DHA, and 1,4-cyclohexadiene (1,4-CHD) and OAT with thioanisole derivatives was investigated, revealing reaction rates comparable to previously reported Mn^{IV}-oxo species.¹⁰³

Scheme 3. Formation of $[Mn^{IV}(O)(dpaq)]^+$ via a stepwise PCET mechanism reported by Paul, Biswas, and coworkers.¹⁰³



Side-on Mn–O₂ intermediates have been shown to be the relevant intermediate in Mn-dependent superoxide dismutase.³¹ In 2016, Kumar, Sastri, Visser and coworkers reported a η^2 side-on Mn^{III} -peroxo complexes with a pentadentate bispidine ligand system (complex **29**) that were reactive toward aldehyde deformylation via a hydrogen atom abstraction (HAA) mechanism rather than nucleophilic addition.¹⁰⁴ This mechanism was further corroborated in a follow-up study that included analysis of a modified bispidine ligand (complex **30**) that altered the orientation of the

pyridine moieties to establish structure-function relationships for the two possible reaction pathways (**Figure 12**).¹⁰⁵ In complex **29**, there are three pyridine groups that are vertically aligned with the z-axis, parallel to the $Mn^{III}-(\eta^2-O_2)$ group, whereas in complex **30** only one pyridine is similarly parallel to the $Mn^{III}-(\eta^2-O_2)$ core and the remaining two pyridines are now coplanar to the in xy-plane.¹⁰⁵ Kinetic analysis with 2-phenylpropionaldehyde (2-PPA) revealed a 5-fold increase in rate with **30** in comparison to **29**, with both showing similar rate-limiting HAA steps.¹⁰⁵ This variation in rate was attributed to the difference in the interaction of the approaching substrate with the $Mn^{III}-(\eta^2-O_2)$ as a result of pyridine group orientation. DFT was also used to elucidate the mechanism, showing that the lowest energy reaction pathway consisted of HAA from the α -position of 2-PAA by $Mn^{III}-(\eta^2-O_2)$, leading to keto-enol tautomerization where the enol-form undergoes nucleophilic attack of the olefin bond.¹⁰⁵

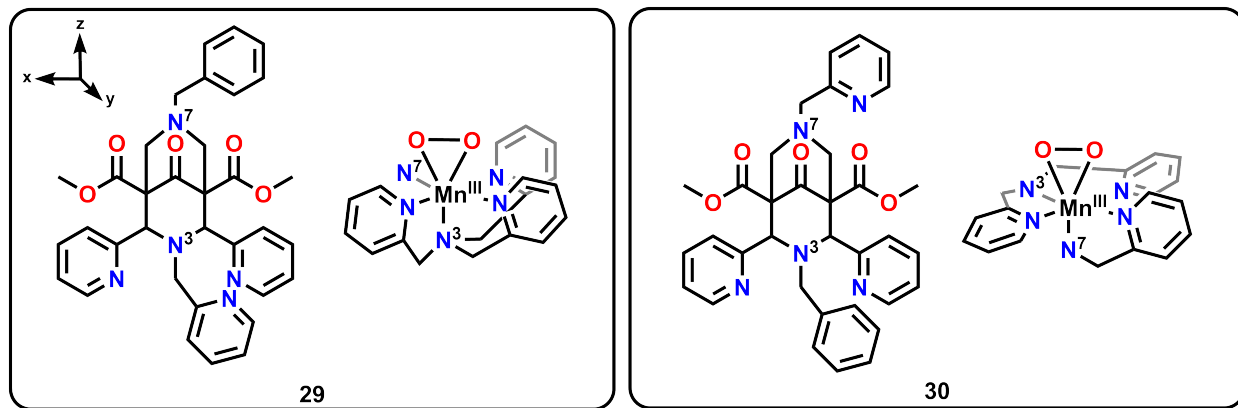
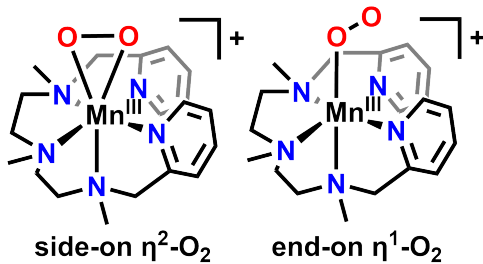


Figure 12. Ligand frameworks and depiction of pyridine group orientation in the inner-coordination sphere for the Mn complexes reported by Kumar, Sastri, Visser and coworkers.¹⁰⁵ Note that the carbonyl-containing backbone connecting N^3 and N^7 has been omitted from the complex for clarity.

A recent report by Dhuri and coworkers established the synthesis, characterization and reactivity of a metastable Mn–peroxo complex that can exist in an end-on η^1 - O_2 or side-on η^2 - O_2 species ($[Mn^{III}(N_3Py_2)(O_2)]^+$, complex **31**) with a non-heme pentadentate ligand, N_3Py_2 (where $N_3Py_2 = N,N'$ -dimethyl- N -(2-(methyl(pyridine-2-ylmethyl)-amino)ethyl)- N' -(pyridine-2-ylmethyl)-ethane-1,2-diamine) (**Figure 13**).¹⁰⁶ This peroxo species $[Mn^{III}(N_3Py_2)(O_2)]^+$ exhibited no oxidation reactivity toward triphenylphosphine, thioanisole, cyclohexene or xanthene, suggesting a lack of electrophilic character. However, addition of 2-PPA to $[Mn^{III}(N_3Py_2)(O_2)]^+$ showed reactivity toward aldehyde deformylation in MeCN solution with acetophenone as the primary product ($88 \pm 2\%$).¹⁰⁶ Addition of cyclohexanecarboxaldehyde also showed rapid reactivity with cyclohexene as a quantitative product ($75 \pm 4\%$).¹⁰⁶ Mechanistic analysis of $[Mn^{III}(N_3Py_2)(O_2)]^+$ 2-PAA as well as

para-substituted benzaldehydes suggested that aldehyde deformylation proceeds via nucleophilic attack of the carbonyl group rather than an initial hydrogen atom abstraction pathway.¹⁰⁶ Dhuri and coworkers suggest that favored nucleophilic attack could be due to ligand flexibility, where initial HAA is prevented by the N_3Py_2 ligand tangling around $\text{Mn}^{\text{III}}-\text{O}_2$.¹⁰⁶



31

Figure 13. Structure of $([\text{Mn}^{\text{III}}(\text{N}_3\text{Py}_2)(\text{O}_2)]^+$ in both side-on $\eta^2\text{-O}_2$ and end-on $\eta^1\text{-O}_2$ conformations reported by Dhuri and coworkers.¹⁰⁶

Metal-superoxo species are proposed to be important intermediates during the reactivity of catechol dioxygenases.^{2,20} In 2019, Lin *et. al* reported an O_2 -derived Mn^{III} -superoxo complex ($\text{Mn}(\text{BDP}^{\text{Br}}\text{P})(\text{O}_2^{\cdot})$, **32**) that was shown to activate the O–H bond of TEMPOH via HAA to form the Mn^{III} -hydroperoxo ($(\text{Mn}^{\text{III}}(\text{BDP}^{\text{Br}}\text{P})(\text{OOH})$, **33**) (Figure 14). Following this, Lin *et. al* studied the ambiphilic character of **32**, showing the formation of a Mn^{IV} -hydroperoxo species ($([\text{Mn}^{\text{IV}}(\text{BDP}^{\text{Br}}\text{P})(\text{OOH})]^+$, **34**) and deformylation of 2-PPA (Figure 14).^{107,108}

Reactivity studies of **32** with 2-PPA in THF at $-80\text{ }^{\circ}\text{C}$ showed competent and selective aldehyde deformylation, generating acetophenone in a 92% yield (Figure 14). Treatment of **32** with trifluoroacetic acid in MeTHF at $-120\text{ }^{\circ}\text{C}$ resulted in the formation of the Mn^{IV} -hydroperoxide, **34**. Interestingly, subsequent addition of a suitable base lead to the reformation of **32**. If a one-electron oxidant was added to the TEMPOH generated Mn^{III} -hydroperoxide **33**, the Mn^{IV} species (**34**) could also be generated; the addition of a one-electron reductant to **34** likewise reformed **33**. Through UV-vis, resonance Raman, and EPR spectroscopies in combination with DFT calculations, Lin *et. al* were able to evaluate the nature of the O–O bond in both the superoxo and hydroperoxo species, as well as propose the Mn^{IV} oxidation state for species **34**.¹⁰⁸ These data demonstrated both the electrophilic and nucleophilic character of **32**, which was attributed to the flexible electronic structure of metal-superoxo species. Upon the addition of a proton source, the partially occupied O–O π^* orbital donates electron density to form the O–H bond in the -OOH moiety, which is compensated by the transfer of an electron from the Mn center.¹⁰⁸

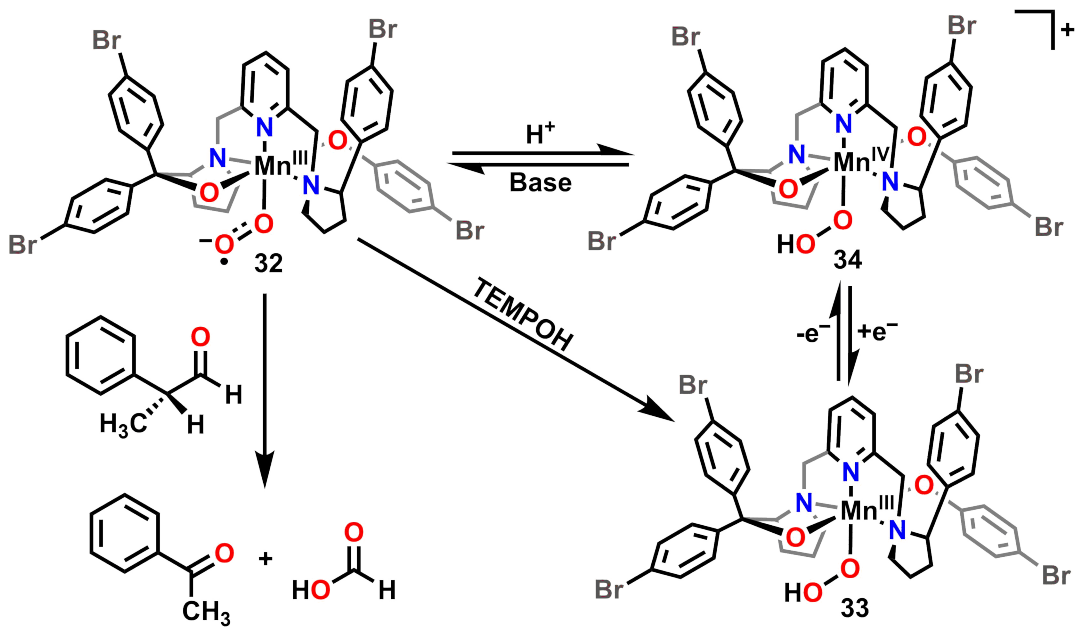


Figure 14. Reactivity of Mn^{III}-superoxo and Mn^{III/IV}-hydroperoxo complexes reported by Lin *et. al.*^{108,109}

Conclusions and Perspectives

Dioxygen is crucial to biological systems and is utilized by nature to perform challenging oxidation reactions during metabolic processes, cellular signaling, and biodegradation of xenobiotic compounds, among others.^{1,2,28} While the field of dioxygen chemistry has been dominated by the study of iron and copper systems, there are a number of important manganese-dependent enzymes that bind and activate O₂. Some examples include manganese-dependent superoxide dismutase, oxalate oxidase, and manganese lipoxygenases.^{28,31} The study of O₂ reactivity at non-heme manganese complexes continues to receive interest in the context of biomimetic systems and substrate oxidation reactions.

Here, we have described recent advances in the development of bioinspired non-heme Mn complexes that activate O₂ and the reactivity of Mn–O species. These studies have established guiding principles for manipulating the ligand scaffold sterically (both in terms of bulk and secondary-sphere interactions) and at the equatorial ligand position to modify the binding and activation of O₂. These alterations of the core complex structure can subsequently be used to establish structure-function relationships established for atom transfer reactivity, although whether or not mechanism changes occur is highly dependent on the nature of the base ligand framework. While reports of non-heme Mn complexes continue to increase, true mimicry of O₂ activation proposed for Mn-dependent enzymes remains elusive. A complicating factor is the

difficulty of isolating and understanding Mn–O intermediates, which are often extremely reactive and do not have the ancillary benefit of element-dependent spectroscopic methods like Mößbauer or nuclear resonance vibrational spectroscopy.^{1,110,111} Further development of model systems for Mn-dependent enzymes will be important to the understanding of enzyme structure and function and lead to the optimization of synthetic Mn complexes that are able to perform oxidation reactions with O₂, as well as reduce it directly in an efficient manner.

Funding Sources

E.N.C. and C.W.M. acknowledge N.S.F. CHE-2102156 and ACS PRF 61430-ND3 for support.

References:

- (1) Sahu, S.; Goldberg, D. P. Activation of Dioxygen by Iron and Manganese Complexes: A Heme and Nonheme Perspective. *J. Am. Chem. Soc.* **2016**, *138* (36), 11410–11428. <https://doi.org/10.1021/jacs.6b05251>.
- (2) Kovaleva, E. G.; Lipscomb, J. D. Versatility of Biological Non-Heme Fe(II) Centers in Oxygen Activation Reactions. *Nat. Chem. Biol.* **2008**, *4* (3), 186–193. <https://doi.org/10.1038/nchembio.71.Versatility>.
- (3) Yoshikawa, S.; Shimada, A. Reaction Mechanism of Cytochrome c Oxidase. *Chem. Rev.* **2015**, *115* (4), 1936–1989. <https://doi.org/10.1021/cr500266a>.
- (4) Zhang, W.; Lai, W.; Cao, R. Energy-Related Small Molecule Activation Reactions: Oxygen Reduction and Hydrogen and Oxygen Evolution Reactions Catalyzed by Porphyrin- and Corrole-Based Systems. *Chem. Rev.* **2017**, *117* (4), 3717–3797. <https://doi.org/10.1021/acs.chemrev.6b00299>.
- (5) Pegis, M. L.; Wise, C. F.; Martin, D. J.; Mayer, J. M. Oxygen Reduction by Homogeneous Molecular Catalysts and Electrocatalysts. *Chem. Rev.* **2018**, *118* (5), 2340–2391. <https://doi.org/10.1021/acs.chemrev.7b00542>.
- (6) Campos-Martin, J. M.; Blanco-Brieva, G.; Fierro, J. L. G. Hydrogen Peroxide Synthesis: An Outlook beyond the Anthraquinone Process. *Angew. Chemie - Int. Ed.* **2006**, *45* (42), 6962–6984. <https://doi.org/10.1002/anie.200503779>.
- (7) Machan, C. W. Advances in the Molecular Catalysis of Dioxygen Reduction. *ACS Catal.* **2020**, *10* (4), 2640–2655. <https://doi.org/10.1021/acscatal.9b04477>.
- (8) Ray, K.; Lee, Y. M.; Nam, W. Dioxygen Activation Chemistry by Synthetic Mononuclear Nonheme Iron, Copper and Chromium Complexes. *Coord. Chem. Rev.* **2017**, *334*, 25–42. <https://doi.org/10.1016/j.ccr.2016.07.006>.
- (9) Solomon, E. I.; Goudarzi, S.; Sutherlin, K. D. O₂ Activation by Non-Heme Iron Enzymes. *Biochemistry* **2016**, *55* (46), 6363–6374. <https://doi.org/10.1021/acs.biochem.6b00635>.
- (10) Jasniewski, A. J.; Que, L. Dioxygen Activation by Nonheme Diiiron Enzymes: Diverse Dioxygen Adducts, High-Valent Intermediates, and Related Model Complexes. *Chem. Rev.* **2018**, *118* (5), 2554–2592. <https://doi.org/10.1021/acs.chemrev.7b00457>.
- (11) Huang, X.; Groves, J. T. Oxygen Activation and Radical Transformations in Heme Proteins and Metalloporphyrins. **2018**. <https://doi.org/10.1021/acs.chemrev.7b00373>.
- (12) Solomon, E. I.; Stahl, S. S. Introduction: Oxygen Reduction and Activation in Catalysis.

Chem. Rev. **2018**, *118* (5), 2299–2301. <https://doi.org/10.1021/acs.chemrev.8b00046>.

- (13) Pau, M. Y. M.; Lipscomb, J. D.; Solomon, E. I. Substrate Activation for O₂ Reactions by Oxidized Metal Centers in Biology. *Proc. Natl. Acad. Sci. U. S. A.* **2007**, *104* (47), 18253–18258.
- (14) Lai, W.; Li, C.; Chen, H.; Shaik, S. Hydrogen-Abstraction Reactivity Patterns from A to Y: The Valence Bond Way. *Angew. Chemie - Int. Ed.* **2012**, *51* (23), 5556–5578. <https://doi.org/10.1002/anie.201108398>.
- (15) Saouma, C. T.; Mayer, J. M. Do Spin State and Spin Density Affect Hydrogen Atom Transfer Reactivity? *Chem. Sci.* **2014**, *5* (1), 21–31. <https://doi.org/10.1039/c3sc52664j>.
- (16) Rittle, J.; Green, M. T. Cytochrome P450 Compound I: Capture, Ch. *Science (80-.)* **2010**, *330* (6006), 933–937. <https://doi.org/10.1126/science.1193478>.
- (17) Andreou, A.; Feussner, I. Lipoxygenases - Structure and Reaction Mechanism. *Phytochemistry* **2009**, *70* (13–14), 1504–1510. <https://doi.org/10.1016/j.phytochem.2009.05.008>.
- (18) Decker, A.; Solomon, E. I. Dioxygen Activation by Copper, Heme and Non-Heme Iron Enzymes: Comparison of Electronic Structures and Reactivities. *Curr. Opin. Chem. Biol.* **2005**, *9* (2), 152–163. <https://doi.org/10.1016/j.cbpa.2005.02.012>.
- (19) Que, L.; Ho, R. Y. N. Dioxygen Activation by Enzymes with Mononuclear Non-Heme Iron Active Sites. *Chem. Rev.* **1996**, *96* (7), 2607–2624. <https://doi.org/10.1021/cr960039f>.
- (20) Costas, M.; Mehn, M. P.; Jensen, M. P.; Que, L. Dioxygen Activation at Mononuclear Nonheme Iron Active Sites: Enzymes, Models, and Intermediates. *Chem. Rev.* **2004**, *104* (2), 939–986. <https://doi.org/10.1021/cr020628n>.
- (21) Kovaleva, E. G.; Neibergall, M. B. Finding Intermediates in the O₂ Activation Pathways of Non-Heme Iron Oxygenases. **2007**, 475–483.
- (22) Blomberg, M. R. A. Mechanism of Oxygen Reduction in Cytochrome c Oxidase and the Role of the Active Site Tyrosine. **2016**. <https://doi.org/10.1021/acs.biochem.5b01205>.
- (23) Liu, J. J.; Diaz, D. E.; Quist, D. A.; Karlin, K. D. Copper(I)-Dioxygen Adducts and Copper Enzyme Mechanisms. *Isr. J. Chem.* **2016**, *56* (9–10), 1–18. <https://doi.org/10.1002/ijch.201600025>.
- (24) Klinman, J. P. Mechanisms Whereby Mononuclear Copper Proteins Functionalize Organic Substrates. **1996**.
- (25) Solomon, E. I.; Heppner, D. E.; Johnston, E. M.; Ginsbach, J. W.; Cirera, J.; Qayyum, M.; Kieber-emmons, M. T.; Kjaergaard, C. H.; Hadt, R. G.; Tian, L. Copper Active Sites in Biology. **2014**.
- (26) Mayilmurugan, R.; Visvaganesan, K.; Suresh, E.; Palaniandavar, M. Iron(III) Complexes of Tripodal Monophenolate Ligands as Models for Non-Heme Catechol Dioxygenase Enzymes: Correlation of Dioxygenase Activity with Ligand Stereoelectronic Properties. *Inorg. Chem.* **2009**, *48* (18), 8771–8783. <https://doi.org/10.1021/ic900969n>.
- (27) Velusamy, M.; Mayilmurugan, R.; Palaniandavar, M. Iron(III) Complexes of Sterically Hindered Tetradentate Monophenolate Ligands as Functional Models for Catechol 1,2-Dioxygenases: The Role of Ligand Stereoelectronic Properties. *Inorg. Chem.* **2004**, *43* (20), 6284–6293. <https://doi.org/10.1021/ic049802b>.
- (28) Zhu, W.; Richards, N. G. J. Biological Functions Controlled by Manganese Redox Changes in Mononuclear Mn-Dependent Enzymes. *Essays Biochem.* **2017**, *61* (2), 259–270.

<https://doi.org/10.1042/EBC20160070>.

- (29) Wennman, A.; Jernerén, F.; Hamberg, M.; Oliw, E. H. Catalytic Convergence of Manganese and Iron Lipoxygenases by Replacement of a Single Amino Acid. *J. Biol. Chem.* **2012**, *287* (38), 31757–31765. <https://doi.org/10.1074/jbc.M112.364331>.
- (30) Wennman, A.; Karkehabadi, S.; Oliw, E. H. Kinetic Investigation of the Rate-Limiting Step of Manganese- and Iron-Lipoxygenases. *Arch. Biochem. Biophys.* **2014**, *555–556*, 9–15. <https://doi.org/10.1016/j.abb.2014.05.014>.
- (31) Sheng, Y.; Abreu, I. A.; Cabelli, D. E.; Maroney, M. J.; Miller, A. F.; Teixeira, M.; Valentine, J. S. Superoxide Dismutases and Superoxide Reductases. *Chem. Rev.* **2014**, *114* (7), 3854–3918. <https://doi.org/10.1021/cr4005296>.
- (32) Schmidt, S. B.; Husted, S. The Biochemical Properties of Manganese in Plants. *Plants* **2019**, *8* (10), 381–395. <https://doi.org/10.3390/plants8100381>.
- (33) Svedružić, D.; Jónsson, S.; Toyota, C. G.; Reinhardt, L. A.; Ricagno, S.; Lindqvist, Y.; Richards, N. G. J. The Enzymes of Oxalate Metabolism: Unexpected Structures and Mechanisms. *Arch. Biochem. Biophys.* **2005**, *433* (1), 176–192. <https://doi.org/10.1016/j.abb.2004.08.032>.
- (34) Scarpellini, M.; Gätjens, J.; Martin, O. J.; Kampf, J. W.; Sherman, S. E.; Pecoraro, V. L. Modeling the Resting State of Oxalate Oxidase and Oxalate Decarboxylase Enzymes. *Inorg. Chem.* **2008**, *47* (9), 3584–3593. <https://doi.org/10.1021/ic701953g>.
- (35) Rheingold, A. L.; Crabtree, R. H.; Brudvig, G. W. A Functional Model for O – O Bond Formation by the O₂ -Evolving Complex in Photosystem II. **1999**, *283* (March), 1524–1528.
- (36) Yano, J.; Yachandra, V.; Divis, P. B.; Berkeley, L. Mn 4 Ca Cluster in Photosynthesis : Where and How Water Is Oxidized to Dioxygen. **2014**, *4205* (1).
- (37) Shirin, Z.; Young, V. G.; Borovik, A. S. Synthesis and Structure of a Mn^{III}(OH) Complex Generated from Dioxygen. *Chem. Commun.* **1997**, *36* (20), 1967–1968. <https://doi.org/10.1039/a703395h>.
- (38) Shook, R. L.; Gunderson, W. A.; Greaves, J.; Ziller, J. W.; Hendrich, M. P.; Borovik, A. S. A Monomeric Mn^{III}-Peroxo Complex Derived Directly from Dioxygen. *J. Am. Chem. Soc.* **2008**, *130* (28), 8888–8889. <https://doi.org/10.1021/ja802775e>.
- (39) Shook, R. L.; Borovik, A. S. Role of the Secondary Coordination Sphere in Metal-Mediated Dioxygen Activation. *Inorg. Chem.* **2010**, *49* (8), 3646–3660. <https://doi.org/10.1021/ic901550k>.
- (40) Coggins, M. K.; Toledo, S.; Shaffer, E.; Kaminsky, W.; Shearer, J.; Kovacs, J. A. Characterization and Dioxygen Reactivity of a New Series of Coordinatively Unsaturated Thiolate-Ligated Manganese(II) Complexes. *Inorg. Chem.* **2012**, *51* (12), 6633–6644. <https://doi.org/10.1021/ic300192q>.
- (41) Coggins, M. K.; Sun, X.; Kwak, Y.; Solomon, E. I.; Rybak-Akimova, E.; Kovacs, J. A. Characterization of Metastable Intermediates Formed in the Reaction between a Mn(II) Complex and Dioxygen, Including a Crystallographic Structure of a Binuclear Mn(III)-Peroxo Species. *J. Am. Chem. Soc.* **2013**, *135* (15), 5631–5640. <https://doi.org/10.1021/ja311166u>.
- (42) Kovacs, J. A. Tuning the Relative Stability and Reactivity of Manganese Dioxygen and Peroxo Intermediates via Systematic Ligand Modification. *Acc. Chem. Res.* **2015**, *48* (10), 2744–2753. <https://doi.org/10.1021/acs.accounts.5b00260>.

(43) Chau Yan Poon, P.; Dedushko, M. A.; Sun, X.; Yang, G.; Toledo, S.; Hayes, E. C.; Johansen, A.; Piquette, M. C.; Rees, J. A.; Stoll, S.; Rybak-akimova, E.; Kovacs, J. A. How Metal Ion Lewis Acidity and Steric Properties Influence the Barrier to Dioxygen Binding, Peroxo O-O Bond Cleavage, and Reactivity. *J. Am. Chem. Soc.* **2019**, *141*, 15046–15057. <https://doi.org/10.1021/jacs.9b04729>.

(44) Parham, J. D.; Wijeratne, G. B.; Mayfield, J. R.; Jackson, T. A. Steric Control of Dioxygen Activation Pathways for MnII Complexes Supported by Pentadentate, Amide-Containing Ligands. *Dalt. Trans.* **2019**, *48* (34), 13034–13045. <https://doi.org/10.1039/c9dt02682g>.

(45) Lieske, L. E.; Hooe, S. L.; Nichols, A. W.; Machan, C. W. Electrocatalytic Reduction of Dioxygen by Mn(III): Mes-Tetra(N-Methylpyridinium-4-Yl)Porphyrin in Universal Buffer. *Dalt. Trans.* **2019**, *48* (24), 8633–8641. <https://doi.org/10.1039/c9dt01436e>.

(46) Baglia, R. A.; Zaragoza, J. P. T.; Goldberg, D. P. Biomimetic Reactivity of Oxygen-Derived Manganese and Iron Porphyrinoid Complexes. *Chem. Rev.* **2017**, *117* (21), 13320–13352. <https://doi.org/10.1021/acs.chemrev.7b00180>.

(47) Neu, H. M.; Baglia, R. A.; Goldberg, D. P. A Balancing Act: Stability versus Reactivity of Mn(O) Complexes. *Acc. Chem. Res.* **2015**, *48* (10), 2754–2764. <https://doi.org/10.1021/acs.accounts.5b00273>.

(48) Liu, W.; Groves, J. T. Manganese Catalyzed C-H Halogenation. *Acc. Chem. Res.* **2015**, *48* (6), 1727–1735. <https://doi.org/10.1021/acs.accounts.5b00062>.

(49) Sorokin, A. B. Phthalocyanine Metal Complexes in Catalysis. *Chem. Rev.* **2013**, *113* (10), 8152–8191. <https://doi.org/10.1021/cr4000072>.

(50) Gennari, M.; Brazzolotto, D.; Pécaut, J.; Cherrier, M. V.; Pollock, C. J.; Debeer, S.; Retegan, M.; Pantazis, D. A.; Neese, F.; Rouzières, M.; Clérac, R.; Duboc, C. Dioxygen Activation and Catalytic Reduction to Hydrogen Peroxide by a Thiolate-Bridged Dimanganese(II) Complex with a Pendant Thiol. *J. Am. Chem. Soc.* **2015**, *137* (26), 8644–8653. <https://doi.org/10.1021/jacs.5b04917>.

(51) Brazzolotto, D.; Cant, G.; Smith-jones, J.; Retegan, M.; Amidani, L.; Faponle, A. S.; Ray, K.; Philouze, C.; Visser, S. P. De; Gennari, M.; Duboc, C. Bioinorganic Chemistry A High-Valent Non-Heme m -Oxo Manganese (IV) Dimer Generated from a Thiolate-Bound Manganese (II) Complex and Dioxygen. **2017**, *2*, 8211–8215. <https://doi.org/10.1002/anie.201703215>.

(52) Gennari, M.; Duboc, C. Bio-Inspired, Multifunctional Metal – Thiolate Motif: From Electron Transfer to Sulfur Reactivity and Small-Molecule Activation. **2020**, No. li. <https://doi.org/10.1021/acs.accounts.0c00555>.

(53) Baldwin, M. J.; Stemmier, T. L.; Penner-hahn, M. L. K. J. E.; Pecoraro, V. L. Structural and Magnetic Effects of Successive Protonations of Oxo Bridges in High-Valent Manganese Dimers. **1994**, No. 3, 11349–11356.

(54) Wu, A. J.; Penner-Hahn, J. E.; Pecoraro, V. L. Structural, Spectroscopic, and Reactivity Models for the Manganese Catalases. *Chemical Reviews.* 2004, pp 903–938. <https://doi.org/10.1021/cr020627v>.

(55) Krewald, V.; Lassalle-kaiser, B.; Iii, T. T. B.; Pollock, C. J.; Kern, J.; Beckwith, M. A.; Yachandra, V. K.; Pecoraro, V. L.; Yano, J.; Neese, F.; Debeer, S. The Protonation States of Oxo-Bridged Mn. **2013**.

(56) Lassalle-kaiser, B.; Iii, T. T. B.; Krewald, V.; Kern, J.; Beckwith, M. A.; Delgado-jaime, M. U.; Schroeder, H.; Alonso-mori, R.; Nordlund, D.; Weng, T.; Sokaras, D.; Neese, F.; Bergmann, U.; Yachandra, V. K.; Debeer, S.; Pecoraro, V. L.; Yano, J. Experimental and

Computational X - Ray Emission Spectroscopy as a Direct Probe of Protonation States in Oxo-Bridged Mn. **2013**.

(57) Lassalle-Kaiser, B.; Hureau, C.; Pantazis, D. A.; Pushkar, Y.; Guillot, R.; Yachandra, V. K.; Yano, J.; Neese, F.; Anxolabéhère-Mallart, E. Activation of a Water Molecule Using a Mononuclear Mn Complex: From Mn-Aquo, to Mn-Hydroxo, to Mn-Oxyl via Charge Compensation. *Energy Environ. Sci.* **2010**, 3 (7), 924–938. <https://doi.org/10.1039/b926990h>.

(58) Ghachoui, S. El; Guillot, R.; Dorlet, P.; Anxolabéhère-Mallart, E.; Aukaloo, A. Influence of Second Sphere Hydrogen Bonding Interaction on a Manganese(II)-Aquo Complex. *Dalt. Trans.* **2012**, 41 (6), 1675–1677. <https://doi.org/10.1039/c1dt11858g>.

(59) Deville, C.; Padamati, S. K.; Sundberg, J.; McKee, V.; Browne, W. R.; McKenzie, C. J. O₂ Activation and Double C-H Oxidation by a Mononuclear Manganese(II) Complex. *Angew. Chemie - Int. Ed.* **2016**, 55 (2), 545–549. <https://doi.org/10.1002/anie.201508372>.

(60) Hooe, S. L.; Rheingold, A. L.; Machan, C. W. Electrocatalytic Reduction of Dioxygen to Hydrogen Peroxide by a Molecular Manganese Complex with a Bipyridine-Containing Schiff Base Ligand. *J. Am. Chem. Soc.* **2018**, 140 (9), 3232–3241. <https://doi.org/10.1021/jacs.7b09027>.

(61) Hooe, S. L.; Machan, C. W. Dioxygen Reduction to Hydrogen Peroxide by a Molecular Mn Complex: Mechanistic Divergence between Homogeneous and Heterogeneous Reductants. *J. Am. Chem. Soc.* **2019**, 141 (10), 4379–4387. <https://doi.org/10.1021/jacs.8b13373>.

(62) Hooe, S. L.; Cook, E. N.; Reid, A. G.; Machan, C. W. Non-Covalent Assembly of Proton Donors and p- Benzoquinone Anions for Co-Electrocatalytic Reduction of Dioxygen. *Chem. Sci.* **2021**, 12 (28), 9733–9741. <https://doi.org/10.1039/d1sc01271a>.

(63) Kovacs, J. A. How Iron Activates O₂. *Science (80-).* **2003**, 299 (5609), 1024–1025. <https://doi.org/10.1126/science.1081792>.

(64) Zaragoza, J. P. T.; Goldberg, D. P. Dioxygen Binding and Activation by Transition Metal Porphyrinoid Complexes. In *Dioxygen-dependent Heme Enzymes*; The Royal Society of Chemistry, 2018; pp 1–36.

(65) Groves, J. T. High-Valent Iron in Chemical and Biological Oxidations. *J. Inorg. Biochem.* **2006**, 100 (4), 434–447. <https://doi.org/10.1016/j.jinorgbio.2006.01.012>.

(66) Guo, M.; Corona, T.; Ray, K.; Nam, W. Heme and Nonheme High-Valent Iron and Manganese Oxo Cores in Biological and Abiological Oxidation Reactions. *ACS Cent. Sci.* **2019**, 5, 13–28. <https://doi.org/10.1021/acscentsci.8b00698>.

(67) Lucas, R. L.; Zart, M. K.; Mukherjee, J.; Sorrell, T. N.; Powell, D. R.; Borovik, A. S. A Modular Approach toward Regulating the Secondary Coordination Sphere of Metal Ions: Differential Dioxygen Activation Assisted by Intramolecular Hydrogen Bonds. *J. Am. Chem. Soc.* **2006**, 128 (48), 15476–15489. <https://doi.org/10.1021/ja069983b>.

(68) Borovik, A. S. Bioinspired Hydrogen Bond Motifs in Ligand Design: The Role of Noncovalent Interactions in Metal Ion Mediated Activation of Dioxygen. *Acc. Chem. Res.* **2005**, 38 (1), 54–61. <https://doi.org/10.1021/ar030160q>.

(69) Shook, R. L.; Borovik, A. S. The Effects of Hydrogen Bonds on Metal-Mediated O₂ Activation and Related Processes. *Chem. Commun.* **2008**, No. 46, 6095–6107. <https://doi.org/10.1039/b810957e>.

(70) Cook, S. A.; Hill, E. A.; Borovik, A. S. Lessons from Nature: A Bio-Inspired Approach to

Molecular Design. *Biochemistry* **2015**, *54* (27), 4167–4180. <https://doi.org/10.1021/acs.biochem.5b00249>.

(71) Cook, S. A.; Borovik, A. S. Molecular Designs for Controlling the Local Environments around Metal Ions. *Acc. Chem. Res.* **2015**, *48* (8), 2407–2414. <https://doi.org/10.1021/acs.accounts.5b00212>.

(72) Coggins, M. K.; Martin-diaconescu, V.; Debeer, S.; Kovacs, J. A. Correlation Between Structural, Spectroscopic, and Reactivity Properties Within a Series of Structurally Analogous Metastable Manganese(III) – Alkylperoxo Complexes. *J. Am. Chem. Soc.* **2013**, *135* (11), 4260–4272.

(73) Rice, D. B.; Massie, A. A.; Jackson, T. A. Manganese-Oxygen Intermediates in O-O Bond Activation and Hydrogen-Atom Transfer Reactions. *Acc. Chem. Res.* **2017**, *50* (11), 2706–2717. <https://doi.org/10.1021/acs.accounts.7b00343>.

(74) Gupta, R.; Taguchi, T.; Lassalle-kaiser, B.; Bominar, E. L.; Yano, J.; Hendrich, M. P. High-Spin Mn – Oxo Complexes and Their Relevance to the Oxygen-Evolving Complex within Photosystem II. **2015**, 1–6. <https://doi.org/10.1073/pnas.1422800112>.

(75) Taguchi, T.; Gupta, R.; Lassalle-Kaiser, B.; Boyce, D. W.; Yachandra, V. K.; Tolman, W. B.; Yano, J.; Hendrich, M. P.; Borovik, A. S. Preparation and Properties of a Monomeric High-Spin MnV-Oxo Complex. *J. Am. Chem. Soc.* **2012**, *134*, 1996–1999.

(76) Taguchi, T.; Stone, K. L.; Gupta, R.; Kaiser-Lassalle, B.; Yano, J.; Hendrich, M. P.; Borovik, A. S. Preparation and Properties of an MnIV-Hydroxide Complex: Proton and Electron Transfer at a Mononuclear Manganese Site and Its Relationship to the Oxygen Evolving Complex within Photosystem II. *Chem. Sci.* **2014**, *5* (8), 3064–3071. <https://doi.org/10.1039/c4sc00453a>.

(77) Barman, S. K.; Jones, J. R.; Sun, C.; Hill, E. A.; Ziller, J. W.; Borovik, A. S. Regulating the Basicity of Metal-Oxido Complexes with a Single Hydrogen Bond and Its Effect on C-H Bond Cleavage. *J. Am. Chem. Soc.* **2019**, *141* (28), 11142–11150. <https://doi.org/10.1021/jacs.9b03688>.

(78) Shirin, Z.; Hammes, B. S.; Young, V. G.; Borovik, A. S. Hydrogen Bonding in Metal Oxo Complexes: Synthesis and Structure of a Monomeric Manganese(III) - Oxo Complex and Its Hydroxo Analogue. *J. Am. Chem. Soc.* **2000**, *122* (8), 1836–1837. <https://doi.org/10.1021/ja993818x>.

(79) Gupta, R.; Borovik, A. S. Monomeric MnIII/II and FeIII/II Complexes with Terminal Hydroxo and Oxo Ligands: Probing Reactivity via O-H Bond Dissociation Energies. *J. Am. Chem. Soc.* **2003**, *125* (43), 13234–13242. <https://doi.org/10.1021/ja030149l>.

(80) MacBeth, C. E.; Gupta, R.; Mitchell-Koch, K. R.; Young, V. G.; Lushington, G. H.; Thompson, W. H.; Hendrich, M. P.; Borovik, A. S. Utilization of Hydrogen Bonds to Stabilize M-O(H) Units: Synthesis and Properties of Monomeric Iron and Manganese Complexes with Terminal Oxo and Hydroxo Ligands. *J. Am. Chem. Soc.* **2004**, *126* (8), 2556–2567. <https://doi.org/10.1021/ja0305151>.

(81) Parsell, T. H.; Behan, R. K.; Green, M. T.; Hendrich, M. P.; Borovik, A. S. Preparation and Properties of a Monomeric Mn IV-Oxo Complex. *J. Am. Chem. Soc.* **2006**, *128* (27), 8728–8729. <https://doi.org/10.1021/ja062332v>.

(82) Parsell, T. H.; Yang, M. Y.; Borovik, A. S. C-H Bond Cleavage with Reductants: Re-Investigating the Reactivity of Monomeric Mn III/IV - Oxo Complexes and the Role of Oxo Ligand Basicity. *J. Am. Chem. Soc.* **2009**, *131* (8), 2762–2763. <https://doi.org/10.1021/ja8100825>.

(83) Bím, D.; Maldonado-Domínguez, M.; Rulísek, L.; Srnec, M. Beyond the Classical Thermodynamic Contributions to Hydrogen Atom Abstraction Reactivity. *Proc. Natl. Acad. Sci. U. S. A.* **2018**, 115 (44), E10287–E10294. <https://doi.org/10.1073/pnas.1806399115>.

(84) Geiger, R. A.; Chattopadhyay, S.; Day, V. W.; Jackson, T. A. A Series of Peroxomanganese(III) Complexes Supported by Tetradentate Aminopyridyl Ligands: Detailed Spectroscopic and Computational Studies. *J. Am. Chem. Soc.* **2010**, 132 (8), 2821–2831. <https://doi.org/10.1021/ja910235g>.

(85) Geiger, R. A.; Chattopadhyay, S.; Day, V. W.; Jackson, T. A. Nucleophilic Reactivity of a Series of Peroxomanganese(III) Complexes Supported by Tetradentate Aminopyridyl Ligands. *Dalt. Trans.* **2011**, 40 (8), 1707–1715. <https://doi.org/10.1039/c0dt01570a>.

(86) Rice, D. B.; Wijeratne, G. B.; Burr, A. D.; Parham, J. D.; Day, V. W.; Jackson, T. A. Steric and Electronic Influence on Proton-Coupled Electron-Transfer Reactivity of a Mononuclear Mn(III)-Hydroxo Complex. *Inorg. Chem.* **2016**, 55 (16), 8110–8120. <https://doi.org/10.1021/acs.inorgchem.6b01217>.

(87) Rice, D. B.; Munasinghe, A.; Grotzmeyer, E. N.; Burr, A. D.; Day, V. W.; Jackson, T. A. Structure and Reactivity of (μ -Oxo)Dimanganese(III,III) and Mononuclear Hydroxomanganese(III) Adducts Supported by Derivatives of an Amide-Containing Pentadentate Ligand. *Inorg. Chem.* **2019**, 58 (1), 622–636. <https://doi.org/10.1021/acs.inorgchem.8b02794>.

(88) Opalade, A. A.; Hessefort, L.; Day, V. W.; Jackson, T. A. Controlling the Reactivity of a Metal-Hydroxo Adduct with a Hydrogen Bond. **2021**. <https://doi.org/10.1021/jacs.1c06199>.

(89) Geiger, R. A.; Leto, D. F.; Chattopadhyay, S.; Dorlet, P.; Anxolabéhère-Mallart, E.; Jackson, T. A. Geometric and Electronic Structures of Peroxomanganese(III) Complexes Supported by Pentadentate Amino-Pyridine and -Imidazole Ligands. *Inorg. Chem.* **2011**, 50 (20), 10190–10203. <https://doi.org/10.1021/ic201168j>.

(90) Leto, D. F.; Ingram, R.; Day, V. W.; Jackson, T. A. Spectroscopic Properties and Reactivity of a Mononuclear Oxomanganese(IV) Complex. *Chem. Commun.* **2013**, 49 (47), 5378–5380. <https://doi.org/10.1039/c3cc00244f>.

(91) Leto, D. F.; Jackson, T. A. Peroxomanganese Complexes as an Aid to Understanding Redox-Active Manganese Enzymes. *J. Biol. Inorg. Chem.* **2014**, 19 (1), 1–15. <https://doi.org/10.1007/s00775-013-1067-4>.

(92) Rice, D. B.; Grotzmeyer, E. N.; Donovan, A. M.; Jackson, T. A. Effect of Lewis Acids on the Structure and Reactivity of a Mononuclear Hydroxomanganese(III) Complex. *Inorg. Chem.* **2020**, 59, 2689–2700. <https://doi.org/10.1021/acs.inorgchem.9b02980>.

(93) Leto, D. F.; Massie, A. A.; Rice, D. B.; Jackson, T. A. Spectroscopic and Computational Investigations of a Mononuclear Manganese(IV)-Oxo Complex Reveal Electronic Structure Contributions to Reactivity. *J. Am. Chem. Soc.* **2016**, 138 (47), 15413–15424. <https://doi.org/10.1021/jacs.6b08661>.

(94) Massie, A. A.; Denler, M. C.; Cardoso, L. T.; Walker, A. N.; Hossain, M. K.; Day, V. W.; Nordlander, E.; Jackson, T. A. Equatorial Ligand Perturbations Influence the Reactivity of Manganese(IV)-Oxo Complexes. *Angew. Chemie* **2017**, 129 (15), 4242–4246. <https://doi.org/10.1002/ange.201612309>.

(95) Singh, P.; Stewart-Jones, E.; Denler, M. C.; Jackson, T. A. Mechanistic Insight into Oxygen Atom Transfer Reactions by Mononuclear Manganese(IV)-Oxo Adducts. *Dalt. Trans.* **2021**, 50 (10), 3577–3585. <https://doi.org/10.1039/d0dt04436a>.

(96) Wijeratne, G. B.; Corzine, B.; Day, V. W.; Jackson, T. A. Saturation Kinetics in Phenolic O-

H Bond Oxidation by a Mononuclear Mn(III)-OH Complex Derived from Dioxygen. *Inorg. Chem.* **2014**, 53 (14), 7622–7634. <https://doi.org/10.1021/ic500943k>.

(97) Cho, K.; Shaik, S.; Nam, W. Theoretical Investigations into C – H Bond Activation Reaction by Nonheme Mn. *J. Phys. Chem. Lett.* **2012**, 3 (19), 2851–2856.

(98) Wu, X.; Seo, M. S.; Davis, K. M.; Lee, Y. M.; Chen, J.; Cho, K. Bin; Pushkar, Y. N.; Nam, W. A Highly Reactive Mononuclear Non-Heme Manganese(IV)-Oxo Complex That Can Activate the Strong C-H Bonds of Alkanes. *J. Am. Chem. Soc.* **2011**, 133 (50), 20088–20091. <https://doi.org/10.1021/ja208523u>.

(99) Sankaralingam, M.; Lee, Y. M.; Karmalkar, D. G.; Nam, W.; Fukuzumi, S. A Mononuclear Non-Heme Manganese(III)-Aqua Complex as a New Active Oxidant in Hydrogen Atom Transfer Reactions. *J. Am. Chem. Soc.* **2018**, 140 (40), 12695–12699. <https://doi.org/10.1021/jacs.8b07772>.

(100) Sharma, N.; Zou, H. B.; Lee, Y. M.; Fukuzumi, S.; Nam, W. A Mononuclear Non-Heme Manganese(III)-Aqua Complex in Oxygen Atom Transfer Reactions via Electron Transfer. *J. Am. Chem. Soc.* **2021**, 143 (3), 1521–1528. <https://doi.org/10.1021/jacs.0c11420>.

(101) Sankaralingam, M.; Lee, Y. M.; Pineda-Galvan, Y.; Karmalkar, D. G.; Seo, M. S.; Jeon, S. H.; Pushkar, Y.; Fukuzumi, S.; Nam, W. Redox Reactivity of a Mononuclear Manganese-Oxo Complex Binding Calcium Ion and Other Redox-Inactive Metal Ions. *J. Am. Chem. Soc.* **2019**, 141 (3), 1324–1336. <https://doi.org/10.1021/jacs.8b11492>.

(102) Karmalkar, D. G.; Sankaralingam, M.; Seo, M. S.; Ezhov, R.; Lee, Y.; Pushkar, Y. N.; Kim, W.; Fukuzumi, S.; Nam, W. A High-Valent Manganese(IV)-Oxo–Cerium(IV) Complex and Its Enhanced Oxidizing Reactivity. *Angew. Chemie* **2019**, 131 (45), 16270–16275. <https://doi.org/10.1002/ange.201910032>.

(103) Biswas, S.; Mitra, A.; Banerjee, S.; Singh, R.; Das, A.; Paine, T. K.; Bandyopadhyay, P.; Paul, S.; Biswas, A. N. A High Spin Mn(IV)-Oxo Complex Generated via Stepwise Proton and Electron Transfer from Mn(III)-Hydroxo Precursor: Characterization and C-H Bond Cleavage Reactivity. *Inorg. Chem.* **2019**, 58 (15), 9713–9722. <https://doi.org/10.1021/acs.inorgchem.9b00579>.

(104) Barman, P.; Upadhyay, P.; Faponle, A. S.; Kumar, J.; Nag, S. S.; Kumar, D.; Sastri, C. V.; de Visser, S. P. Deformylation Reaction by a Nonheme Manganese(III)-Peroxo Complex via Initial Hydrogen-Atom Abstraction. *Angew. Chemie - Int. Ed.* **2016**, 55 (37), 11091–11095. <https://doi.org/10.1002/anie.201604412>.

(105) Cantú Reinhard, F. G.; Barman, P.; Mukherjee, G.; Kumar, J.; Kumar, D.; Sastri, C. V.; De Visser, S. P. Keto-Enol Tautomerization Triggers an Electrophilic Aldehyde Deformylation Reaction by a Nonheme Manganese(III)-Peroxo Complex. *J. Am. Chem. Soc.* **2017**, 139 (50), 18328–18338. <https://doi.org/10.1021/jacs.7b10033>.

(106) Narulkar, D. D.; Ansari, A.; Vardhaman, A. K.; Harmalkar, S. S.; Lingamallu, G.; Dhavale, V. M.; Sankaralingam, M.; Das, S.; Kumar, P.; Dhuri, S. N. A Side-on Mn(II)-Peroxo Supported by a Non-Heme Pentadentate N3Py2ligand: Synthesis, Characterization and Reactivity Studies. *Dalt. Trans.* **2021**, 50 (8), 2824–2831. <https://doi.org/10.1039/d0dt03706k>.

(107) Lin, Y. H.; Cramer, H. H.; Van Gastel, M.; Tsai, Y. H.; Chu, C. Y.; Kuo, T. S.; Lee, I. R.; Ye, S.; Bill, E.; Lee, W. Z. Mononuclear Manganese(III) Superoxo Complexes: Synthesis, Characterization, and Reactivity. *Inorg. Chem.* **2019**, 58 (15), 9756–9765. <https://doi.org/10.1021/acs.inorgchem.9b00767>.

(108) Lin, Y. H.; Kutin, Y.; Van Gastel, M.; Bill, E.; Schnegg, A.; Ye, S.; Lee, W. Z. A

Manganese(IV)-Hydroperoxo Intermediate Generated by Protonation of the Corresponding Manganese(III)-Superoxo Complex. *J. Am. Chem. Soc.* **2020**, *142* (23), 10255–10260. <https://doi.org/10.1021/jacs.0c02756>.

- (109) Lin, Y.; Cramer, H. H.; Gastel, M. Van; Tsai, Y.; Chu, C.; Kuo, T.; Lee, I.; Ye, S.; Bill, E.; Lee, W. Mononuclear Manganese(III) Superoxo Complexes: Synthesis, Characterization, and Reactivity. *Inorg. Chem.* **2019**, *58* (15), 9756–9765. <https://doi.org/10.1021/acs.inorgchem.9b00767>.
- (110) Gordon, J. B.; Vilbert, A. C.; Dimucci, I. M.; MacMillan, S. N.; Lancaster, K. M.; Moënne-Loccoz, P.; Goldberg, D. P. Activation of Dioxygen by a Mononuclear Nonheme Iron Complex: Sequential Peroxo, Oxo, and Hydroxo Intermediates. *J. Am. Chem. Soc.* **2019**, *141* (44), 17533–17547. <https://doi.org/10.1021/jacs.9b05274>.
- (111) Scheidt, W. R.; Li, J.; Sage, J. T. What Can Be Learned from Nuclear Resonance Vibrational Spectroscopy: Vibrational Dynamics and Hemes. *Chem. Rev.* **2017**, *117* (19), 12532–12563. <https://doi.org/10.1021/acs.chemrev.7b00295>.